Gamma Reconstruction — Model-Driven Approach

[Note] Model diagnostic figures — run python visualise_pixel.py --pixel <IDX> to regenerate Figures 1 and 2 for any pixel in the source grid (0 – pixel_count−1). Example: python visualise_pixel.py --pixel 2 --anode 37 --output-prefix readme
>

[Note] Metric comparison figures — run python visualise_metrics.py to regenerate metrics_fig2 through metrics_fig5 referenced in the second half of this document.

Camera Design and the 6×6 Problem

The detector grid and coded-aperture (CA) mask are similarly sized, so at 36 of the possible source positions the CA shadow falls grid-on-grid onto the detector. Every image reconstruction technique tried so far finds peaks at those 36 positions — the physics forces them there regardless of algorithm. This makes the camera effectively a 6×6-pixel device in the absence of any countermeasure.

The multiple-CA-position technique breaks the grid-on-grid association by rotating the CA mask through several angular positions before each acquisition frame. This introduces part-anode shadows that carry sub-grid spatial information, enabling an effective pixel count well beyond 6×6.

The Model

The reconstruction model translates detector anode counts into a 70×70 gamma image. Each pixel in that image represents a 3D vector radiating from the camera — if a radioactive source exists anywhere along that vector, it should appear at the corresponding pixel position. The image plane is fixed at a chosen camera-to-image-plane distance.

For each of the 1 225 candidate positions in the 35×35 source grid the model pre-calculates, for every anode and every CA rotation angle, the **expected anode power** (the share of counts that would arrive at that anode via the CA if a source of unit strength were located on that pixel's 3D vector). After scoring, the 35×35 score map is cubic-spline up-sampled to a 70×70 output image. Comparing model predictions against the measured anode counts is how the camera decides whether — and how strongly — a source is present at each candidate position.

Scoring a Single Pixel: the Per-Anode View

For each candidate pixel the model evaluates one (model_power, observed_count) pair per anode per CA rotation. The chart below shows anode 37 across the 7 CA positions for pixel 2 in the 35×35 source grid — the anode with the strongest positive via-CA response at this pixel.

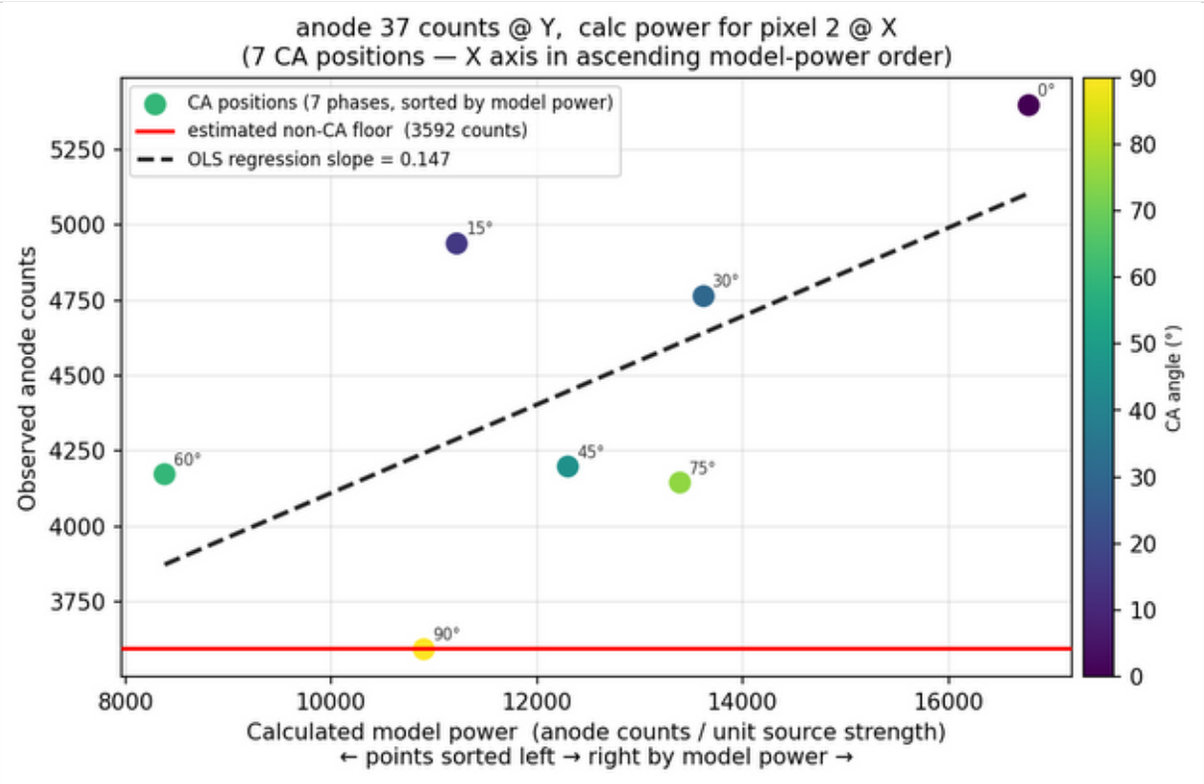

Single-anode example: anode 37 counts vs model power for pixel 2

Figure 1 — Anode 37 counts (Y axis) plotted against the calculated model power for pixel 2 (X axis) at each of the 7 CA positions. Each point is colour-coded by CA rotation angle. The red horizontal line estimates the non-CA count floor — photons reaching this anode by paths that do not pass through the CA (scatter, background, direct leakage). The dashed OLS line shows the positive slope: observed counts rise with model power, indicating source activity on the 3D vector for pixel 2. A flat or negative relationship would indicate no source at that pixel.

> [Note] Regenerate for any pixel: python visualise_pixel.py --pixel <IDX> The script auto-selects the anode with the strongest positive slope.

What the slope means

The slope of the relationship between model power and observed counts is the key quantity. Because the CA modulates how many counts arrive at each anode as a function of rotation angle, the slope can only be non-zero if via-CA gamma rays are present. The Y-intercept (the non-CA floor) is irrelevant — it reflects background radiation and direct leakage that are the same regardless of source position.

In a fully calibrated detector the via-CA slope should be **identical for all 64 anodes** for the same pixel, even though each anode has its own non-CA floor.

Combining All Anodes: the Central Visualisation

Because all anodes share the same via-CA slope for a given pixel, the data from all 64 anodes can be overlaid on a single plot. This gives **7 CA positions × 64 anodes = 448 (model power, observed count) pairs** for each candidate pixel, from which a single regression slope is derived.

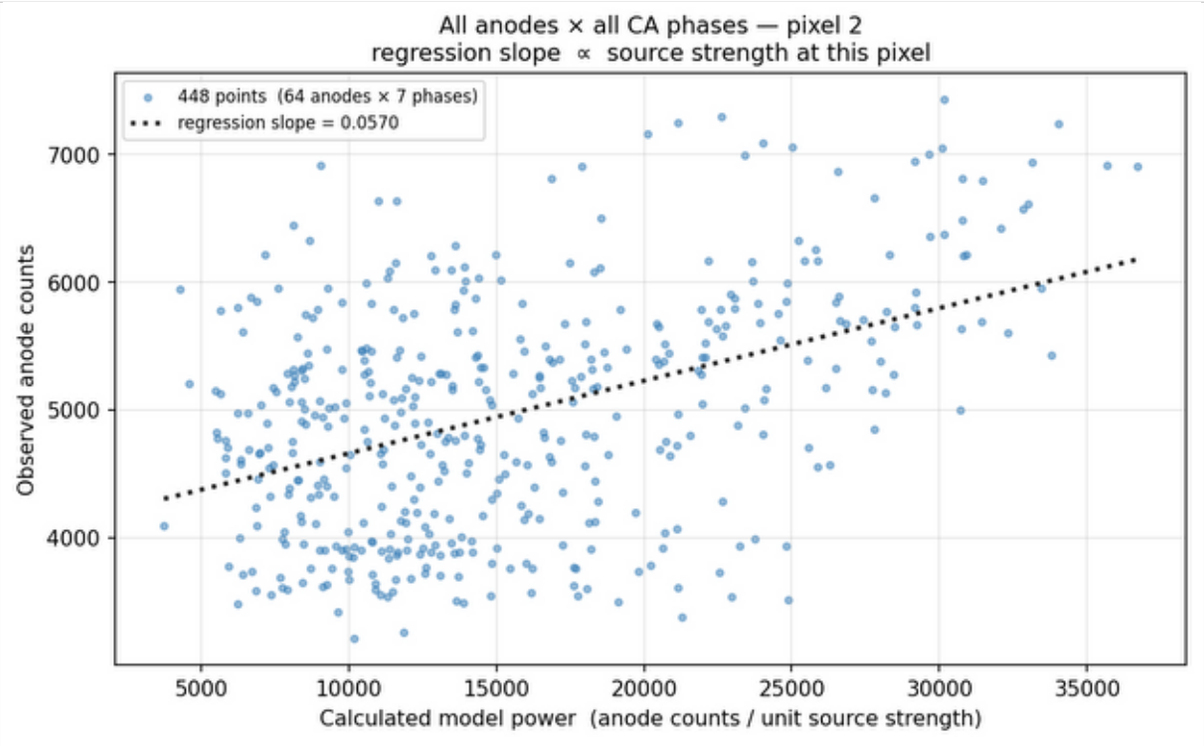

All-anode regression scatter: 448 data points for pixel 2

Figure 2 — All 64 anodes × 7 CA positions plotted together for pixel 2 (observed anode counts on Y, calculated model power on X). Each anode contributes a cluster of 7 points, offset vertically from other anodes by its own non-CA floor. The dotted line is the single least-squares regression slope fitted across the entire 448-point dataset — ignoring per-anode Y-offsets because they are nuisance parameters. A positive slope (as shown here) indicates source activity on this pixel's 3D vector; a near-zero or negative slope indicates no source. Repeating this score for all 1 225 pixels and up-sampling the resulting slope map produces the reconstructed gamma image.

The scatter is large because each anode carries its own non-CA floor (Y-offset), but since all anodes share the same via-CA slope the regression is still well determined. Pooling evidence from all 64 anodes into a single slope score is why the multi-anode approach improves localisation compared with using any single anode's correlation.

Choosing the Figure of Merit

The scatter plot above is a useful conceptual illustration: if a source is present on pixel p's 3D vector, observed counts should be high wherever the model predicts high power, giving a positive slope. The ideal score for pixel p would be an OLS regression that fits one common slope across all 64 anodes while absorbing each anode's independent background floor (non-CA floor) as its own intercept — a fixed-effects model.

The code implements a simpler approximation: it builds a single length-448 vector of all (model_power, observed_count) pairs and applies a similarity metric to the two vectors as-is, without profiling out the 64 per-anode background floors. This means the per-anode Y-offsets are included in the comparison, which can reduce sensitivity relative to a true fixed-effects slope. The choice of FOM determines both how well the background contamination is suppressed and how robust the score is to noise.

For each candidate pixel the code builds two vectors of length n_channels × n_phases = 64 × 7 = 448. For every detector channel and every active CA phase the model-predicted count is placed at index logical_channel × n_phases + phase_offset; the corresponding measured count goes to the same index in the observed vector. The chosen FOM is then applied to these two length-448 vectors. The pixel whose model best matches the observation receives the highest score; the 35×35 score map is cubic-spline up-sampled to the 70×70 output image.

Why Pearson Correlation Is Not Ideal

The Pearson correlation coefficient was the original FOM. It is defined as:

```
r = cov(O, M) / (σ_O · σ_M)
```

where O is the observed vector and M is the model prediction vector. While familiar and easy to compute, it has several properties that make it a poor choice here.

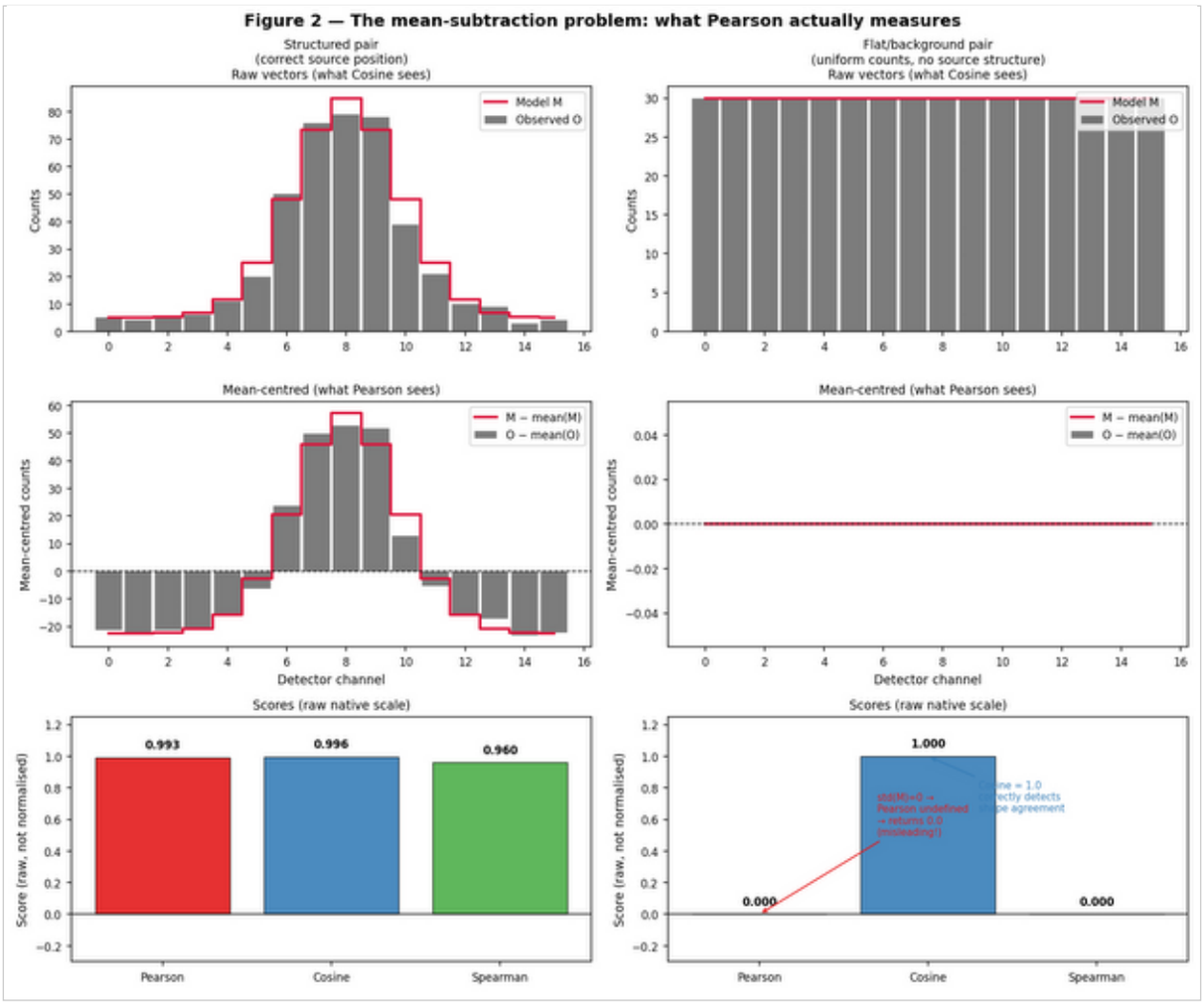

Mean-subtraction problem

Figure 3 — What Pearson actually operates on vs what Cosine operates on. For a flat/uniform pair (right column), mean-subtraction leaves only noise, making std(M) = 0 so Pearson returns 0 even though the shapes agree perfectly. Cosine correctly returns 1.0.

---

1. Mean-subtraction distorts sparse or imbalanced phase data

Pearson centres both vectors around their respective means before computing the inner product. In coded-aperture gamma imaging the observed counts per phase vary substantially — some rotation angles place the CA mask over high-sensitivity detector elements and others do not. Mean-subtraction can flip the sign of low-count phases (making a phase with genuinely few counts appear as a negative contribution) and can inflate the apparent agreement between a model that predicts near-zero counts for some phases and an observation that also has near-zero counts, when what has actually been measured is just background noise.

2. Incorrect noise model

Photon detection is a counting process governed by Poisson statistics: the variance of a count is equal to its expected value, not a fixed constant. Pearson implicitly assumes Gaussian errors with uniform variance (ordinary least-squares geometry in the normalised space). This mismatch means high-count bins and low-count bins are treated as equally reliable, even though high-count bins carry proportionally more statistical information. Rare but large fluctuations in low-count channels therefore disproportionately affect the score.

3. Scale invariance is inappropriate here

Pearson is invariant to multiplicative rescaling of either vector. In practice this means a model predicting a uniform, featureless count distribution can score highly against an observed vector that is also approximately uniform, even though no useful shape information has been matched — Pearson can mistake flat agreement for structured agreement.

4. Sensitivity to outliers

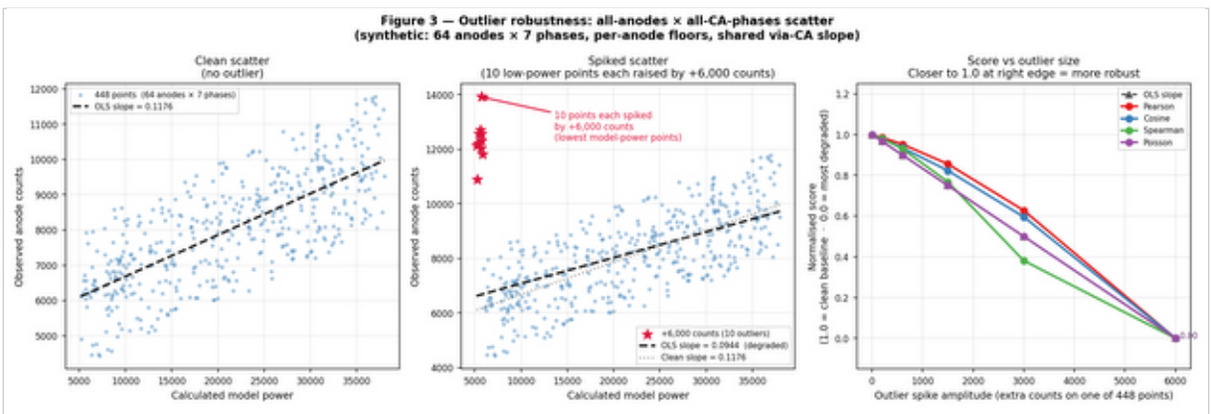

Outlier robustness

Figure 4 — Synthetic all-anodes × all-CA-phases scatter (64 anodes × 7 phases = 448 points, per-anode floors, shared via-CA slope). Left: clean scatter. Middle: ten lowest-model-power points each spiked by +6 000 counts — the OLS slope is pulled from 0.118 to 0.094 and the crimson stars are visibly above the trend. Right: normalised score vs spike size (1.0 = clean baseline). Cosine is the most robust; Spearman degrades more slowly than Pearson; Poisson is the most sensitive.

A detector channel with an anomalously high count — due to a cosmic-ray event or electronic noise — inflates the variance term in Pearson's denominator, dragging down the correlation for otherwise well-matched vectors. Because the spiked points have low model power (left side of the scatter), they create large rank mismatches that also hurt Spearman, but less severely. Cosine similarity is least affected because the dominant L2 norm is spread across all 448 components and a handful of outliers barely rotate the observed-vector direction.

Alternative Metrics

Three alternative figures of merit are implemented, selectable via --reconstruction-metric.

Cosine Similarity (--reconstruction-metric cosine)

```
cos(O, M) = (O · M) / (‖O‖ · ‖M‖)
```

Cosine similarity is the normalised dot product — equivalently, the dot product of the two unit vectors:

```
cos(O, M) = (O/‖O‖) · (M/‖M‖)
```

Geometrically this is the **projection of the observation's direction vector onto the model's direction vector**. Both vectors live in the $8\times8\times7 = 448$- dimensional count space (64 anodes × 7 CA phases). For each candidate pixel in the 35×35 source grid the model supplies a pre-computed direction vector $\hat{M} = M/\|M\|$; cosine similarity asks how closely the current shadowgram points in that same direction — 1 meaning perfect alignment (source present), 0 meaning orthogonal (source absent).

For strictly non-negative count data the result lies in $[0, 1]$, making it straightforward to interpret. Crucially it does not subtract the mean, so the full raw flux distribution across all phases contributes directly.

Why it improves on Pearson:

- No mean-subtraction. Phases with genuinely high counts contribute a large dot-product term; phases with near-zero counts contribute near zero. The metric therefore directly rewards matching the flux distribution shape across phases, which is precisely what localises the source.
- Naturally scale-invariant (via ℓ_2 normalisation) in a way that preserves the relative phase structure, unlike Pearson's mean-centred normalisation.
- Robust against overall count-rate offsets (e.g., changes in source activity between acquisition segments).

Limitation: Like Pearson, it does not respect the Poisson variance structure — all channels are weighted equally regardless of their statistical uncertainty.

Spearman Rank Correlation (--reconstruction-metric spearman)

Spearman rank correlation \rho is computed by replacing each element of both vectors with its rank within that vector, and then computing Pearson correlation on the rank-transformed values.

Why it improves on Pearson:

- Outlier robustness. An anomalously large channel value is mapped to a high rank,

so its magnitude no longer dominates the calculation. When the outlier also has low model power (low X rank) the rank mismatch is still penalised, but less severely than Pearson's variance-inflation effect — see Figure 4 right panel.

- Monotone rather than strictly linear agreement. The reconstruction quality relies

on the phases being ordered by count rate in a way that mirrors the model prediction; Spearman captures this ordering faithfully even when the relationship is non-linear (e.g., due to detector saturation or non-uniform flat-field corrections).

- Retains a familiar [-1, 1] range and zero-under-independence interpretation.

Limitation: Rank transformation loses absolute count magnitude information. Two candidate positions whose models predict different amounts of flux modulation but the same rank ordering will receive identical Spearman scores.

Profile Poisson Log-Likelihood (--reconstruction-metric poisson)

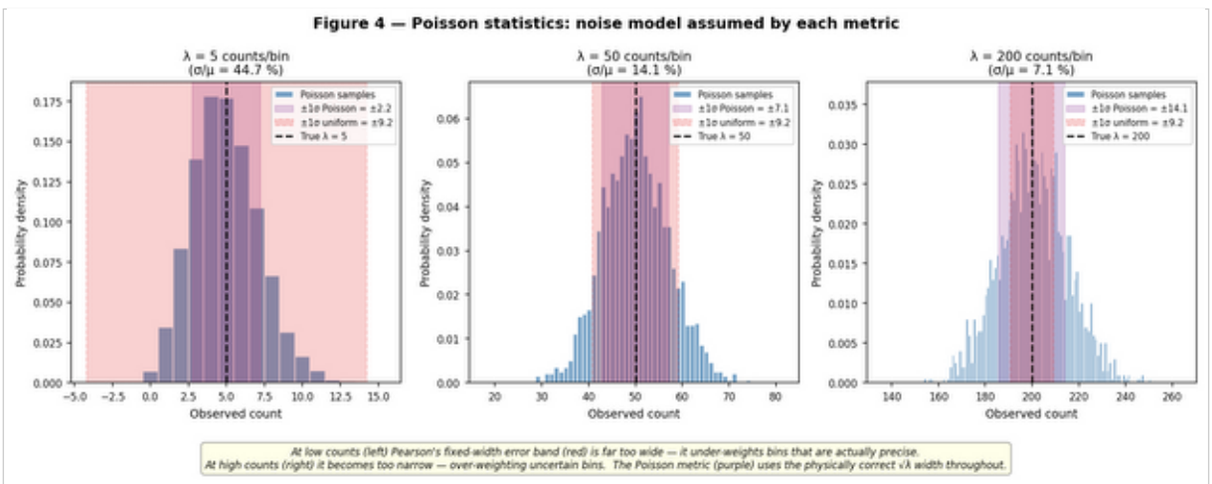

Poisson noise model

Figure 5 — Poisson count distributions at three intensity levels. The Poisson-correct ±1σ band (purple) scales with √λ. Pearson's implicit uniform error band (red) is far too wide at low counts (under-weighting precise measurements) and too narrow at high counts (over-weighting noisy ones).

This is the statistically optimal figure of merit for photon-counting data.

The Poisson likelihood for observing counts O_i when the expected count is λ_i is:

```
L = ∏_i  exp(−λ_i) · λ_i^{O_i} / O_i!
```

The model prediction for pixel position p gives expected counts proportional to M_i. Because the absolute source intensity is unknown, a single scale factor α is introduced: λ_i = α M_i. The maximum-likelihood value of α is:

```
α̂ = Σ O_i / Σ M_i
```

Substituting back into the log-likelihood yields the profile log-likelihood:

```
ll_profile = Σ_i [ O_i · log(α̂ M_i) − α̂ M_i ]
```

which depends only on the shape of the model vector, not its overall normalisation. The score stored in the reconstruction image is this quantity divided by the number of valid terms (so that images accumulated over different numbers of active phases remain comparable).

Why this is more optimal than Pearson:

- Correct noise model. The score is derived directly from the Poisson probability

of the observed data given the model shape. Bins with high expected counts contribute proportionally more to the score, correctly reflecting their greater statistical weight.

- Scale-free by construction. The unknown source intensity is profiled out

analytically, with no need to normalise both vectors post-hoc.

- Sensitivity to shape, not offset. The log term O_i · log(λ_i) rewards having

the model concentrate predicted counts where observed counts are high; the −λ_i penalty discourages over-predicting empty channels.

- Asymptotically efficient. Among all unbiased statistics, the likelihood-ratio test

(of which this is a component) achieves the minimum possible variance in the large-sample limit (Cramér–Rao bound).

Limitation: The score is in log-likelihood units, which are not bounded to [0, 1] or [-1, 1], so the reconstructed image values are less immediately interpretable without normalisation. The metric also requires λ_i > 0 (channels where the model predicts zero counts are excluded from the sum).

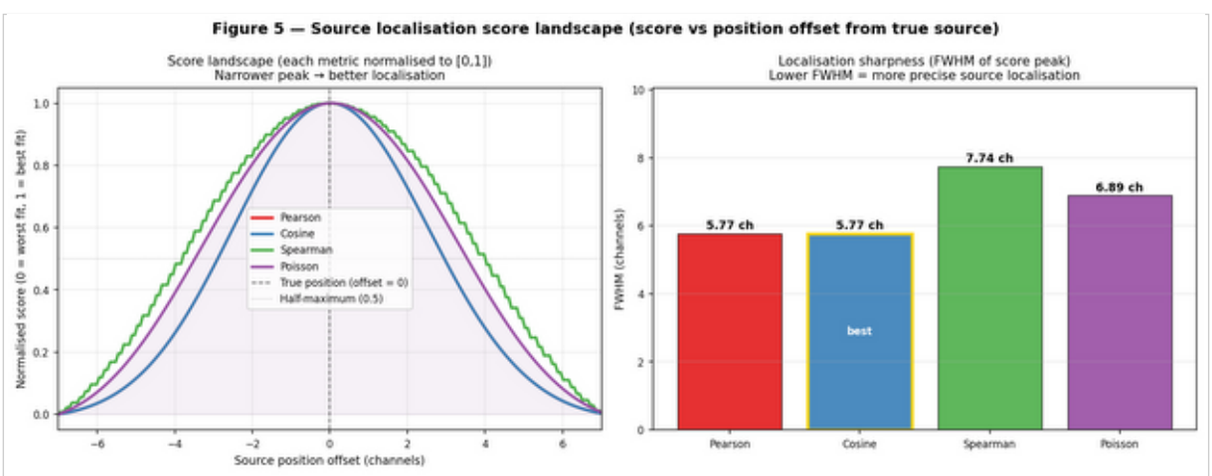

Score landscape

Figure 6 — Score vs source-position offset from the true location (toy 1D model, Poisson-noisy observation). The narrower the peak the more precisely the metric can localise the source. FWHM bars (right) give a quantitative summary; the metric with the lowest FWHM is highlighted.

Metric Comparison Summary

Property	Pearson	Cosine	Spearman	Poisson
Mean-subtracted	Yes	No	Yes (ranks)	No
Correct noise model (Poisson)	No	No	No	Yes
Outlier robust	No	Moderate	Yes	Moderate
Scale-invariant	Yes	Yes	Yes	Yes (profiled)
Bounded output	[-1,1]	[0,1]	[-1,1]	Unbounded
Optimal for count data	No	No	No	Yes

The current default is cosine. For data with well-calibrated flat-field corrections and sufficient statistics per phase, poisson is expected to give the best source localisation because it is the only metric derived from the true generative model of the data. spearman is recommended when detector noise or occasional high-count outliers are suspected. pearson is retained for reproducibility comparisons with prior results only.